# Extraction and Grouping of Surface Features for 3D Mapping

Blair Howarth, Mark Whitty, Jayantha Katupitiya, Jose Guivant
School of Mechanical and Manufacturing Engineering, UNSW, Sydney, Australia

***Abstract*— This paper describes new methods to extract surface features and then group them together. This is required for a planar surface fitting approach that uses both range and vision information to build 3D surface maps for a wall climbing robot. A modified incremental 2D line segmentation approach is presented along with the use of image lines for clustering to improve the performance. A method for verifying the linearity of the line segments was also presented to filter out non-linear line segments so that the planar assumption is not violated during surface fitting. An approach to group these features together was provided based on the physical surfaces that generated them. Both experimental and simulated data sets were used to validate these methods. The results showed that the proposed modifications improved the robustness of the line segmentation by minimising the rate of false positives and the non-linear line segments were successfully filtered out. The feature grouping was performed conservatively and a very low rate of false groupings was seen as a result. These all combine to improve the plane fitting accuracy as the major cause of fitting error is false positive segmentations.**

## I. INTRODUCTION

The ability to map its environment in some manner is an important step towards autonomous behaviour for a mobile robot. The robot needs to develop some understanding of its environment so that it can perform its designated functions. Many successful robotic mapping approaches have been developed for 2D use for a range of different robots [1]. These are, however, unsuitable for robots which move in 3D space, such as aerial or wall climbing robots.

Wall climbing robots can walk on, climb over or move through most obstacles in their way because they are small and highly agile. This allows them to undertake a variety of useful tasks in environments which are typically difficult or dangerous for a human or wheeled/aerial robot to access. Due to their 3D motion, these robots require a 3D mapping system to allow navigation. This allows the robot to operate autonomously which is a requirement for use in enclosed or confined environments where the lack of line-of-sight makes remote control operation unreliable to impossible [2].

As these robots are usually small in size, their mapping capabilities are generally limited or non-existent [3]. Most require external assistance for mapping and navigation due to their lack of onboard sensing or computational hardware [4]. Because of this, no suitable method has been developed that fully meets the onboard 3D mapping needs of a typical small wall climbing robot. Other robotic mapping methods are either limited to 2D use, are not real time using onboard hardware or they consist of an unsuitable map representation.

A 3D mapping approach was recently presented by the authors [5] to fit planar surfaces for use by a small wall climbing robot, shown in Fig. 1(a). This mapping method used the sparse data acquisition and the fusion of range and vision data to fit planar surfaces to groups of features. An example 3D map generated using this method is shown in Fig. 1(b). The range data was used to fit infinite planes with the image information being used to determine the planar polygon boundaries. This feature based approach was taken to reduce the computational burden of the surface mapping approach. This was important to allow real time operation using the limited computational resources available to wall climbing robots due to payload restrictions.

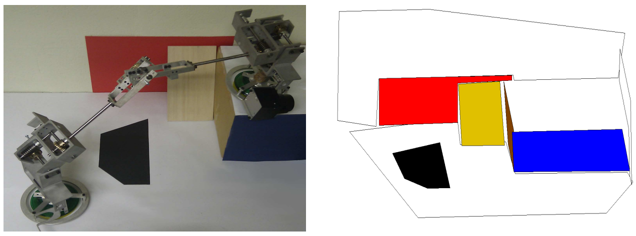

(a) Wall climbing robot. (b) Example of generated 3D map.

Fig. 1. Robot and 3D mapping system requiring surface features.

This paper describes in detail the methods used by [5] to extract range and image features and group together those from the same surface. The extraction of image features is described in Section II followed by the range feature extraction in Section III. After the feature extraction stage, an approach to group the features together is detailed in Section IV. This is followed by experimental results and a discussion of the performance of the proposed methods in Section V.

## II. IMAGE FEATURE EXTRACTION

Image features are extracted from a low resolution ($176 \times 287$ pixels) colour CMOS camera. These will be used during surface fitting to define the planar polygon boundaries. These features should correspond to the corners and edges of physical surface. A Canny edge detector [6] was used followed by a scale space corner detector [7]. While any other edge detector could be used, Canny edge detection generally gives good results. The image lines were required to possess a minimum number of supporting points and be linear. This improved the robustness of the extraction, especially against false texture edges.

A graphical structure was used where the image corners are the graph nodes and the image lines are directed edges. Each image line is used twice during the feature grouping stage as every physical edge has two sides corresponding to the two physical surfaces it separates. This graph representation is compact and allows for easy searching of connected features for the feature grouping process. Further details of this grouping can be found in Section IV.

## III. RANGE FEATURE EXTRACTION

A Hokuyo URG04-LX Laser Range Finder (LRF) is used to acquire 2D range scans. These can be converted into 2D cartesian coordinates on the laser plane and line segments can then be extracted. These line segments can be used for plane fitting once they have been converted into 3D space.

### A. 2D Line Segmentation

A good quality segmentation of the laser range finder measurements into linear segments is very important for the success of the plane fitting approach. It is important that the segmentation is accurate and so it should be performed conservatively. False positive points in the line segments are undesirable and should be minimised, even at the expense of a higher rate of false negative segmentation. As the surface boundaries are not dependent on the laser segment edges, it is not necessary for them to be detected perfectly.

There are several commonly used algorithms for 2D line segmentation including incremental line growing, recursive splitting and edge finding approaches [8][9]. The incremental approach was chosen and several modifications were proposed to improve its robustness and accuracy, possibly at the expense of segment endpoint accuracy. This modified incremental segmentation algorithm is shown in Algorithm 1 and the modifications are explained below.

**Algorithm 1** Modified Incremental Segmentation.

```
start ← i
end ← i + 4
while !validLine(fitLine(start:end)) do
   start ← start+1
   end ← end+1
end while
while validLine(fitLine(start:end)) do
   if pointsOnLine(end+1:end+3) then
      end ← end+3
   else
      return fitLine(start+1:end-1)
   end if
end while
return fitLine(start+1:end-1)
```

The segmentation starts with a small number of consecutive points that form an initial candidate line. Each increment adds the next one or more points and then refits a 2D line. A test condition, such as the distance of the points to the line, is used to verify the linearity of the point set to determine if the line segment is still linear or not.

In contrast to the standard algorithm, the next candidate points are tested before adding them to the line segment so they have no influence on the line parameters until they are integrated. This allows a change in direction to be detected earlier because it reduces the tendency of the incremental approach to follow a curve in the data. Several such advanced points are tested and integrated into the line segment before refitting to improve the speed of the algorithm.

Another modification is to ignore the first and last points in each extracted segment as these are commonly segmented into the wrong line. In the case where a discarded endpoint was in fact correctly segmented, little is lost during plane fitting unless the total number of points is small.

### B. Pre Segmentation - Image Line Clustering

A common technique to improve the performance of the line segmentation is to first split the range scan into point clusters where large range jumps exist. This can improve both speed and accuracy [8]. Image lines are used here instead of range jumps.

It is easy to find the corresponding laser bearing in the specific case where the LRF scans perpendicular to the Y camera axis, the vertical offset between the two sensor apertures is small, and the horizontal offset is small. The laser scan line will project onto the image as a horizontal line running through the principal point $v_0$, as seen in Fig. 2. Any image lines that intersect this line will imply that the laser range scan should be split at that point. As the two sensors are aligned horizontally, the horizontal bearing of a feature in one sensor is directly transferable into the other.

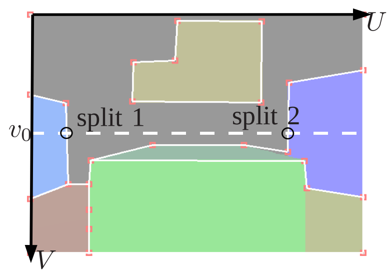


Fig. 2. Laser line projection for pre-splitting using image lines.

Each image line, represented by its two endpoints $\mathbf{p_1}$ and $\mathbf{p_2}$ in $u$,$v$ coordinates, is checked for this intersection. For each intersecting image line, the $u$ value at the intersection must be interpolated using (1) to determine the splitting point.

$$u_i = \frac{(v_0 - v_1)(u_2 - u_1)}{v_2 - v_1} + u_1 \qquad (1)$$

This process provides a set of values $u = u_1 \dots u_N$ which can be converted into an angular bearing using (2) to determine the splitting points in the raw LRF data. The measurement index $i$ can found from (2) where $R$ is the LRF angular resolution and $N$ is the total number of measurements taken, assuming the scan is centred.

$$i = \frac{\theta_i}{R} + \frac{N}{2} \qquad \text{where} \qquad \theta_i = \tan^{-1}\left(\frac{u_0 - u_i}{f_u}\right) \qquad (2)$$

*1) General Case:* In the general case where the horizontal or vertical sensor offset is significant, more work is required to find the corresponding LRF bearing for each image pixel on the horizontal line. Note that if the offset is large or the LRF does not scan parallel to the horizontal axis of the camera then the horizontal line assumption is invalid.

It is not possible anymore to directly correspond the horizontal bearings between sensors because of the sensor offsets, as seen in Fig. 3. The laser points that have been projected onto the image in $u, v$ coordinates track across the image in an increasing fashion due to the consecutive nature of the LRF scanning process. Thus it becomes a 1D search problem to correspond the splitting points $x_i$ with the appropriate laser bearing index.

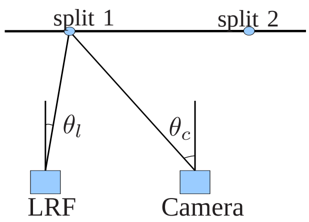


Fig. 3. General case with sensor offset.

A similar problem was tackled by Ellekilde [10] but they required a 2D, rather than 1D, search which is a more complicated problem. Care should be taken to ensure that correct camera calibration has been performed and that any spurious texture based image features are minimised. This approach also assumes that all intersecting image edges are extracted and are linear. Some edges may be missing due to failure of the image feature extraction. This is not a big issue, however, as the line segmentation should still find those segment edges anyway.

### C. *Linearity Verification of Line Segments*

The plane fitting method described in this work relies on the assumption that the surface features were generated by planar surfaces. The linear segmentation of the laser range scans can sometimes fit piecewise linear segments to non-planar surfaces. This can lead to the generation of poor quality planar surfaces.

An example of such false line segments is shown in Fig. 4 below. Both line segments are shown in red with their supporting points in blue and they have identical scale. The line segment in Fig. 4(a) is from a linear surface. Fig. 4(b) shows a nonlinear surface and a tell-tale curve can be seen.

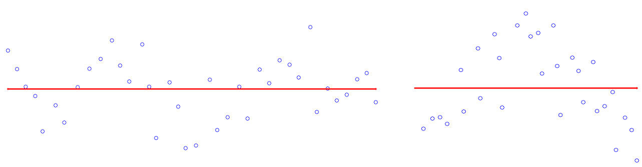

(a) Linear segment. (b) Nonlinear segment.

Fig. 4. Linearity verification of line segments.

If a line segment was generated from a planar surface then it is reasonable to expect that the variance of those points should lie almost exclusively along the direction of that line. It stands to reason that a non-planar surface being approximated by a linear segment should have a relatively higher variance in the orthogonal direction.

An orthogonal least squares line fit can be performed using Principal Components Analysis (PCA). It finds the eigenvectors of the covariance matrix of the points. Each eigenvalue corresponds directly to the proportion of total variance present along the direction of its corresponding eigenvector. The first eigenvalue $\lambda_1$ provides a measure of the variance along the line while $\lambda_2$ gives the variance orthogonal to the line.

A variance based metric is proposed using these two eigenvalues, as seen in (3). It is the percentage of the variance explained by the orthogonal direction of the line, with lower values indicating higher linearity.

$$\left(\frac{\lambda_2}{\lambda_1 + \lambda_2}\right) \times 100 < \Delta_l \tag{3}$$

A cutoff threshold $\Delta_l$ was used to filter out the non-linear segments. Its value can vary depending on the relative importance of minimising false positives or false negatives. Two test sets of linear and non-linear line segments were used to evaluate this metric, as seen below in Table I.

TABLE I

LINE SEGMENTATION - LINEARITY VERIFICATION

| $\Delta_l$ | True + | False + |
|---|---|---|
| <1.5% | 80% | 0% |
| <2.0% | 90% | 10% |
| <2.5% | 100% | 30% |

A value of 1.5% gave no false positives. It was able to successfully filter out all the nonlinear segments but several legitimate linear segments were also removed. Higher thresholds reduced the rate of false negatives but began to introduce more false positives which are generally undesirable. In this work a value of 1.5% was chosen to minimise the number of false line segments passing through to the plane fitting stage. The effect of a false plane being fit to non-planar data could potentially be catastrophic whereas missing a single line segment is relatively less likely to cause the plane fitting to fail due to the redundancy of multiple scans.

## IV. FEATURE GROUPING

The image and range features extracted in Sections II and III are of no use individually for plane fitting. It is necessary to associate those features generated by the same physical surface in a process called feature grouping. The proposed method is a pure grouping method and involves no feature matching. It is not necessary for the same image features to be detected in each and every image during the grouping stage. This is a major benefit if the feature extraction proves difficult in certain environments.

Several approaches to grouping image features have been previously suggested based on various criteria. Spatial grouping [11] involves grouping image features that are close to each other. Perceptual grouping [12] relies on the idea that images line with similar properties, such as collinearity, are unlikely to have been generated by chance. The grouping of laser line segments is not usually performed for plane fitting, with the exception of scan line grouping [13]. This uses region growing for fitting planes to dense range data by first segmenting each individual 2D LRF scan into line segments.

### A. Overview of Proposed Feature Grouping Approach

None of the existing grouping approaches are suitable as they cannot handle multiple feature types. A new feature grouping approach is proposed here which combines three separate grouping steps.

1) Extract laser and image features from new 2D scan.
2) **(Laser-Image Grouping)** Associate each laser line segment that intersects a surface with the image features that surround it on the new scan.
3) **(Image-Image Grouping)** Associate together all image features that surround a common surface.
4) **(Laser-Laser Grouping)** Associate the grouped features from steps 2 and 3 with those of previous 2D scans by matching coplanar line segments.
5) Get the next scan and go to Step 1.

An example of grouped features is shown below in Fig. 5. The three images show the grouped features for the front of the green box from three consecutive scans. It consists of three laser lines segments (red) and 22 image lines (white).

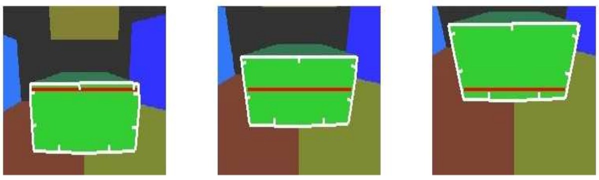

Fig. 5. Example of grouped features from the same physical surface.

### B. Laser-Image Feature Grouping

The laser range and image features are associated with each other by finding the image lines that surround the laser line segment. Each laser line can be projected onto an image as a 2D line in $u$,$v$ coordinates. The image lines that are intersected by the end points of the laser line segment are selected as candidates for matching, pending verification tests such as colour matching. Each image line is represented by two image end points ($p_1, p_2$) and likewise each projected laser line segment is represented by ($p_3, p_4$), as in Fig. 6. This task now becomes a 2D line intersection problem.

Assuming the projected laser line is horizontal, the intersection parameter $a$ can be found using (4).

$$a = \frac{(v_3 - v_1)}{(v_2 - v_1)} \tag{4}$$

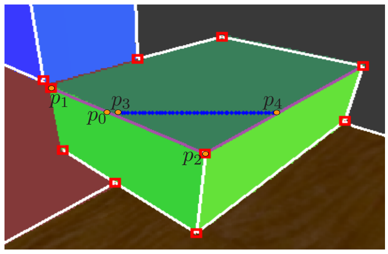


Fig. 6. Image points used to calculate intersection of projected laser line segment (blue) with potential image lines (purple).

The distance in pixels from the end of the laser line segment to the intersection point $p_0$ is found using (5). For a match to be achieved this distance should be less than some threshold $\Delta_d$. This ensures that only image lines intersecting near the end of each line segment are grouped, allowing for some error in the feature extraction locations. This distance $d$, in image pixels, is found in (5).

$$d = |a(u_4 - u_3)| < \Delta_d \tag{5}$$

The $a$ parameter can be used to determine where the image line segment is intersected by the laser line segment. Any value within the range $0 > a > 1$ means that the intersection lies within the image line segment. If this condition holds then that image line is deemed to be a match to he laser line segment. It is also necessary to determine which side is the inside of the image line as it is the image line sides that are actually grouped, not the image lines. The inside is the side that is on the same surface as the laser line segment. Once this has been determined, it remains to check that the colour descriptors match. These consist of the average and variance of the raw RGB values. A weighted vector distance is used to calculate a match.

### C. Image-Image Feature Grouping

Once an image line side has been grouped to a laser line segment, it is used as a seed line to group further image lines. The image feature graph is traversed in both directions from the seed line to find connected image lines corresponding to the same physical surface. Three criteria are used to determine which image line sides, if any, should be also grouped.

**Grouping Criteria:** The desired image line side should meet all criteria below.

1) Be connected to an image line currently in the group.
2) Be the first image line radiating from the corner on the same side of the line.
3) Have the same colour descriptor for the corresponding line side.

If these three grouping criteria are satisfied then the chosen image line side is added to the group and then becomes the next seed image line. After a successful grouping, this process continues to traverse the graph until the grouping is terminated when no suitable ungrouped image line remains. This method to group connected image lines within a single image is reliant on having an accurate image feature graph and good selection of image seed lines.

### D. Laser-Laser Feature Grouping

Finally, the laser line segments are grouped together. They are used to group the features across images which eliminates the need for feature matching or tracking, as in other grouping approaches.

Each new laser line segment will either be associated with an existing group or will spawn a new feature group. It is projected onto the new image and the intersecting image seed lines are extracted, as described in the laser-image grouping above. If these seed lines have already been grouped, then the laser line segment is also associated with that same group if several criteria are met. The colour descriptors should match and there should exist some continuous image path image between the new and existing line segments.

The new line segment should also be coplanar with those already in the group and this should be tested prior to planar surface fitting. If this is violated then a different surface fitting approach will be required.

## V. RESULTS

Two experimental data sets and a simulated data set were acquired and used to validate the feature extraction and grouping methods previously introduced. They were acquired by taking a series of 2D LRF scans and camera images of the environments shown in Fig. 7. The two real scenes were identical setups except the second scene also contained three additional non-planar surfaces. This was used to compare the segmentation performance with a more cluttered scene and the ability to recognise nonlinear line segments. In total there were eighteen 2D scans from the two real datasets resulting in 87 line segments and eleven 2D scans from the simulated environment with 55 line segments being extracted.

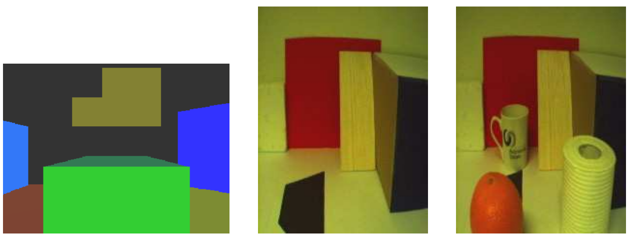

(a) Simulated environment. (b) Real environment. (c) Real environment with some nonplanar surfaces.

Fig. 7. Scenes used for laser line segmentation testing.

### A. Range Segmentation Results

The 2D line segmentation results using the simulated and real range data are shown in Table II below. This compares the segmentation of the basic modified incremental approach with the addition of the image line pre splitting step. Each line segment was classified as a true positive segment if it corresponded to a linear surface. False positive segments were only tested for the second real scene. This measured the number of non-linear segments generated as a percentage of the number of true linear segments present. The remaining columns show the percentage of undersegmented surfaces and the EdgeError shows the segments which contained at least one endpoint that was more than one bearing outside the true endpoint range bearing.

TABLE II

RANGE SEGMENTATION RESULTS

| Data Set | Method | True + | False + | Under Seg. | Edge Error |
|---|---|---|---|---|---|
| Sim | Basic | 82% | N/A | 11% | 7% |
| Sim | Pre Split | 98% | N/A | 2% | 4% |
| Real 1 | Basic | 75.0% | N/A | 25.0% | 31.8% |
| Real 1 | Pre Split | 100% | N/A | 0% | 6.8% |
| Real 2 | Basic | 81.4% | 200% | 11.6% | 23.2% |
| Real 2 | Pre Split | 90.7% | 157% | 0% | 7.0% |

The basic modified incremental method successfully segmented 75-82% of the true laser line segments for the three data sets. By introducing the image line pre splitting, this increased to over 90%. More importantly, the rates of under segmentation and edge error reduced significantly. This was the aim of the presented modifications as it is more important that the 2D segmentation minimises the number of false positive points rather than attempting to find the segment edges exactly. These edges are not used to find the planar polygon boundaries in [5], unlike other plane fitting methods.

The second real scan in Table II above showed a high rate of false positive segments being generated. This was caused by the three non-planar surfaces shown in Fig. 7(c) being approximated by piecewise linear segments. The results of introducing the linear verification method of Section III-C are shown below in Table III.

TABLE III

RANGE SEGMENTATION RESULTS WITH NONLINEAR VERIFICATION

| Segmentation | True + (old) | True + (new) | False + (old) | False + (new) |
|---|---|---|---|---|
| Basic | 81.4% | 69.8% | 200% | 29% |
| Pre Splitting | 90.7% | 81.4% | 157% | 0% |

The addition of this extra segmentation stage was able to successfully filter out the majority of the line segments generated from nonlinear surfaces. The true positive detection rate declined but the false positive rate was significantly reduced and was completely eliminated when pre splitting was also used. This is important when plane fitting is used in [5] as attempting to fit planes to non-planar data will seriously degrade the surface accuracy.

### B. Feature Grouping Results

The proposed feature grouping method was evaluated using the simulated scene and the first real scene shown above. For each 3D scan a series of metrics were compiled to determine the grouping performance. Table IV shows the results the grouping for the simulated and experimental scenes. True groups corresponded correctly to an actual surface while false groups did not. Fittable groups were those true groups that had enough features to allow a planar surface to be fit.

TABLE IV
RESULTS OF SURFACE GROUPING

| Data Set | Surfaces | True Groups | False Groups | Fittable Groups |
|---|---|---|---|---|
| Sim | 46 | 91% | 1 | 81% |
| Real | 25 | 80% | 4 | 100% |

For the real data, 80% of the true physical surfaces had a corresponding feature group, with only a small number of false groups being generated. All these true groups were able to have a good surface fit to them as they contained at least two laser line segments and enough image features to generate a polygon boundary. Similar results were seen for the simulated data. Overall, the grouping failures were mostly caused by the sparse scanning resolution used to acquire the raw data and the image feature extraction process, rather the grouping method itself.

The accuracy of the grouping of individual features is shown below in Table V. True groupings show the number of features grouped to the correct surface while false groupings were those features that were assigned incorrectly.

TABLE V
RESULTS OF GROUPING IMAGE AND LASER FEATURES

| Data Set | Image Lines | True Group | False Group | Laser Lines | True Group | False Group |
|---|---|---|---|---|---|---|
| Sim | 1977 | 59.3% | 0.1% | 142 | 90.2% | 0% |
| Real | 1144 | 48.0% | 2.2% | 91 | 80.2% | 1.1% |

The low rate of false groupings at 1-2% is important in achieving good planar fitting accuracy. This was caused by the conservative nature of the process which also meant that many features were not grouped to any surface. This is not a critical issue due to the redundancy of the mapping approach which allows surface features to be observed in multiple scans. It is more important to minimise false groupings as these can lead to poor performance if they are not handled during the grouping stage.

## VI. CONCLUSIONS

This paper has presented the extraction and grouping of image and range features for use in planar surface fitting.

The 2D range scans were linearly segmented using several modifications to the existing incremental segmentation approach. The addition of a pre-segmentation splitting step using image edges was shown to be beneficial. This lead to an improvement in the accuracy of the segmentation edges. A method was also proposed which verified that each line segment was generated from a linear surface. It successfully filtered out those line segments that were caused by non-planar surfaces being segmented in a piece-wise fashion. This is important because of the planar assumption inherent to the surface fitting process.

The proposed surface fitting approach requires the extracted features to be grouped together and a method to perform this was presented. This method successfully grouped features from 80% of surfaces in the test environments and the rate of false positive groupings was very low, at just over 2%. This will allow for accurate surfaces to be fit to the majority of the planar surfaces in an environment.

## VII. ACKNOWLEDGMENTS

This work is supported in part by the ARC Centre of Excellence programme, funded by the Australian Research Council (ARC) and the New South Wales State Government.

## REFERENCES

[1] S. Thrun, “Robotic mapping: A survey,” *Exploring artificial intelligence in the new millennium*, pp. 1–35, 2002.
[2] J. Casper and R. Murphy, “Human-robot interactions during the robot-assisted urban search and rescue response at the world trade center,” *Systems, Man, and Cybernetics, Part B: Cybernetics, IEEE Transactions on*, vol. 33, no. 3, pp. 367 – 385, 2003.
[3] W. Meiting, T. Shili, D. Junjian, and Y. Liwen, “Complete coverage path planning of wall-cleaning robot using visual sensor,” *Electronic Measurement and Instruments, 2007. ICEMI ’07. 8th International Conference on*, pp. 4–159 –4–164, aug. 2007.
[4] J. Xiao, “Cooperative wall-climbing robots in 3d environments for surveillance and target tracking,” tech. rep., City College of the City University of New York, 2009.
[5] B. Howarth, J. Katupitiya, J. Guivant, and A. Szwec, “Novel robotic 3d surface mapping using range and vision fusion,” *Intelligent Robots and Systems (IROS), 2010 IEEE/RSJ International Conference on*, pp. 1539–1544, 2010.
[6] J. Canny, “A computational approach to edge detection,” *Readings in computer vision: issues, problems, principles, and paradigms*, vol. 184, 1987.
[7] X. He and N. Yung, “Corner detector based on global and local curvature properties,” *Optical Engineering*, vol. 47, p. 057008, 2008.
[8] V. Nguyen, S. Gächter, A. Martinelli, N. Tomatis, and R. Siegwart, “A comparison of line extraction algorithms using 2d range data for indoor mobile robotics,” *Autonomous Robots*, vol. 23, no. 2, pp. 97–111, 2007.
[9] A. Siadat, A. Kaske, S. Klausmann, M. Dufaut, and R. Husson, “An optimized segmentation method for a 2d laser-scanner applied to mobile robot navigation,” *Proceedings of the 3rd IFAC symposium on intelligent components and instruments for control applications*, 1997.
[10] L. Ellekilde, S. Huang, J. Valls Miro, and G. Dissanayake, “Dense 3d map construction for indoor search and rescue,” *Journal of Field Robotics*, vol. 24, no. 1-2, p. 71, 2007.
[11] Y.-L. Chang and J. K. Aggarwal, “Line correspondences from cooperating spatial and temporal grouping processes for a sequence of images,” *Computer Vision and Image Understanding*, vol. 67, no. 2, pp. 186 – 201, 1997.
[12] R. Mohan and R. Nevatia, “Using perceptual organization to extract 3d structures,” *IEEE Transactions on Pattern Analysis and Machine Intelligence*, vol. 11, pp. 1121–1139, 1989.
[13] X. Jiang and H. Bunke, “Fast segmentation of range images into planar regions by scan line grouping,” *Machine Vision and Applications*, vol. 7, no. 2, pp. 115–122, 1994.